https://doi.org/10.5194/tc-2020-234
Preprint. Discussion started: 2 September 2020


The Cryosphere Discussions
Open Access
EGU

# Radiocarbon dating of alpine ice cores with the dissolved organic carbon (DOC) fraction

Ling Fang[1,2,3], Theo M. Jenk[1,3,*], Thomas Singer[1,2,3], Shugui Hou[4,5], Margit Schwikowski[1,2,3]

*Corresponding author: Theo M. Jenk (theo.jenk@psi.ch)

[1]Laboratory for Environmental Chemistry, Paul Scherrer Institute, CH-5232 Villigen PSI, Switzerland

[2]Department of Chemistry and Biochemistry, University of Bern, CH-3012 Bern, Switzerland

[3]Oeschger Centre for Climate Change Research, University of Bern, CH-3012 Bern, Switzerland

[4]School of Geographic and Oceanographic Sciences, Nanjing University, Nanjing, 210023, China

[5]School of Oceanography, Shanghai Jiao Tong University, Shanghai 200240, China

https://doi.org/10.5194/tc-2020-234
Preprint. Discussion started: 2 September 2020


The Cryosphere Discussions
Open Access
EGU

## Abstract

High-alpine glaciers are valuable archives of past climatic and environmental conditions. The interpretation of the preserved signal requires a precise chronology. Radiocarbon ($^{14}C$) dating of the water-insoluble organic carbon (WIOC) fraction has become an important dating tool to constrain the age of ice cores from mid-latitude and low-latitude glaciers. However, in some cases this method is restricted by the low WIOC concentration in the ice. In this work, we report first $^{14}C$ dating results using the dissolved organic carbon (DOC) fraction, which is present at concentrations of at least a factor of two higher than the WIOC fraction. We evaluated this new approach by comparison to the established WIO$^{14}C$ dating based on parallel ice core sample sections from four different Eurasian glaciers covering an age range of several hundred to around 20'000 years. $^{14}C$ dating of the two fractions yielded comparable ages with WIO$^{14}C$ revealing a slight, barely significant, systematic offset towards older ages. Our data suggests this to be caused by incompletely removed carbonate from mineral dust ($^{14}C$ depleted) contributing to the WIOC fraction. While in the DOC extraction procedure inorganic carbon is monitored to ensure complete removal, the average removal efficiency for WIOC samples was here estimated to be ~96%. We did not find any indication of in-situ production systematically contributing to DO$^{14}C$ as suggested in a previous study. By using the DOC instead of the WIOC fraction for $^{14}C$ dating, the required ice mass can be reduced to typically ~250 g, yielding a precision of ±200 years or even better if sample sizes typically required for WIO$^{14}C$ dating are used. This study shows the potential of pushing radiocarbon dating of ice forward even to remote and Polar Regions, where the carbon content in the ice is particularly low, when applying the DOC fraction for $^{14}C$ dating.

https://doi.org/10.5194/tc-2020-234
Preprint. Discussion started: 2 September 2020


The Cryosphere Discussions
Open Access
EGU

## 1 Introduction

For a meaningful interpretation of the recorded paleoclimate signals in ice cores from glacier archives, an accurate chronology is essential. Annual layer counting, supported and tied to independent time markers such as the 1963 nuclear fallout horizon evident by a peak maximum in tritium or other radioisotopes, or distinct signals from known volcanic eruptions in the past is the fundamental and most accurate technique used for ice core dating. However, for ice cores from high-alpine glaciers this approach is limited to a few centuries only, because of the exceptional strong thinning of annual layers in the vicinity of the bedrock. Most of the current analytical techniques do not allow high enough sampling resolution for resolving seasonal fluctuations or detecting distinct single events in this depth range. Ice flow models, which are widely used to retrieve full depth age scales (e.g. Nye, 1963; Bolzan, 1985; Thompson et al., 2006), also fail in the deepest part of high-alpine glaciers due to the complex bedrock geometry. Even with 3D models, which require extensive geometrical data, it is highly challenging to simulate a reasonable bottom age (e.g. Licciulli et al., 2020). This emphasizes the need for an absolute dating tool applicable to the oldest, bottom parts of cores from these sites.

Radioactive isotopes contained in the ice offer the opportunity to obtain absolute ages of an ice sample. For millennial scale ice cores, $^{14}C$ dating is the technique of choice. With a half-life of 5370 years, dating in the age range from ~250 years to up to ten half-life times is theoretically possible, covering the time range accessible by alpine glaciers in the vast majority of cases (Uglietti et al., 2016). $^{14}C$ dating of water insoluble organic carbon (WIOC) from glacier ice has become a well-established technique for ice core dating. Samples of >10 µg WIOC can be dated with reasonable uncertainty (10-20%), requiring less than 1 kg of ice from typical mid-latitude and low-latitude glaciers (Jenk et al., 2007; Jenk et al., 2009; Sigl et al., 2009; Uglietti et al., 2016). However, the low WIOC concentration in some glaciers and in Polar Regions, with the corresponding large demands of ice mass puts a limit to this application. Concentrations of dissolved organic carbon (DOC) in glacier ice are a factor of 2-8 higher compared to typical WIOC concentrations (Legrand et al., 2007; Legrand et al., 2013; May et al., 2013, Fang et al., in prep.). Using the DOC fraction for $^{14}C$ dating could therefore reduce the required amount of ice or, for sample sizes similar to what would be needed for $^{14}C$ dating by WIOC, improve the achievable analytical (dating) precision which strongly depends on the absolute carbon mass even for state-of-the-art micro-radiocarbon dating. The underlying hypothesis of applying the DOC fraction for $^{14}C$ dating is the same as for the WIO$^{14}C$ dating

https://doi.org/10.5194/tc-2020-234
Preprint. Discussion started: 2 September 2020


approach (Jenk et al., 2006; Jenk et al., 2007; Jenk et al., 2009). DOC in ice is composed of atmospheric water soluble organic carbon (WSOC) contained in carbonaceous aerosol particles and organic gases taken up during precipitation (Legrand et al., 2013). WSOC is formed in the atmosphere by oxidation of gases emitted from the biosphere or from anthropogenic sources (Legrand et al., 2013; Fang et al. in prep.) and subsequent condensation of the less volatile products. Carbonaceous aerosols transported in the atmosphere can be deposited on a glacier by wet and dry deposition. Before the industrial revolution, these organic carbon species, then entirely of non-fossil origin, contain the contemporary atmospheric $^{14}C$ signal of the time when the snow deposited on the glacier (Jenk et al., 2006). In view of the analytical precision achievable with this method, the turn-over time from atmospheric $CO_2$ to deposited aerosol is negligible (Fang et al., in prep.).

For analyzing DO$^{14}C$ in ice cores, one of the major limitations is the relatively low extraction efficiency ranging from 64% (Steier et al., 2013) to 96% (May et al., 2013; Fang et al., 2019) and the high risk of sample contamination (Legrand et al., 2013) potentially introduced during drilling, storage, and sample processing. A first attempt to use DOC for $^{14}C$ dating of ice samples was conducted by May (2009) using a set-up for a combined analysis of both, the DOC and WIOC fraction with subsequent radiocarbon micro-analysis. However, these first results suggested a potential in-situ production of $^{14}C$ in the DOC fraction based on the obtained super modern F$^{14}C$ values (i.e. F$^{14}C$ values higher than ever observed in the recent or past ambient atmosphere). Building on these initial findings, May (2009) questioned the applicability of the DOC fraction for radiocarbon dating. Although the in-situ $^{14}C$ production of $^{14}CO$ and $^{14}CO_2$ in air bubbles contained in polar ice has been studied thoroughly and is rather well understood (Van de Wal et al., 1994; Lal et al., 1997; Smith et al., 2000), possible mechanisms of $^{14}C$ in-situ formation in organic compounds seem far less likely and have not been investigated to date (Woon, 2002). To further explore the potential of DO$^{14}C$ for dating ice, a DOC extraction setup for radiocarbon analyses was designed and built at the Paul Scherrer Institut (PSI). In order to minimize potential contamination, the entire system is protected from ambient air by inert gas (helium) flow or vacuum. To maximize the oxidation efficiency, the PSI DOC methodology applies an ultraviolet (UV) photochemical oxidation step supported by addition of Fenton's reagent. The setup has been characterized by a high extraction efficiency of 96% and a low overall process blank being superior in the resulting blank to sample ratio compared to other systems (Fang et al., 2019). The system can handle samples with volumes of up to ~350 mL allowing $^{14}C$ analysis on samples with DOC

https://doi.org/10.5194/tc-2020-234
Preprint. Discussion started: 2 September 2020


concentrations as low as 25 µg/kg. In this study, we evaluate $^{14}C$ dating with the DOC fraction by comparing to results from the well- established WIO$^{14}C$ dating method. This is not only analytically highly challenging, but also because of the very limited availability of the precious sampling material needed in a rather large quantity (> 500 g) and ideally covering a wide range of ages from a few hundred to several thousands of years. Here, such samples from four different Eurasian glaciers were analyzed in parallel.

## 2 Sample preparation and $^{14}C$ analysis

To validate the DOC $^{14}C$ dating technique, a total of 17 samples from the deep parts of ice cores from the four glaciers Colle Gnifetti, Belukha, Chongce (Core 1), and Shule Nanshan (SLNS) were selected (Figure 1). The high-alpine glacier Colle Gnifetti is located in the Monte Rosa massif of the Swiss Alps, close to the Italian border. A 76 m long core was retrieved from the glacier saddle in September 2015 at an altitude of 4450 m asl. (45°55'45.7''N, 7°52'30.5''E). Four samples were selected from the bottom 4 m (72-76 m) closest to bedrock. The Belukha core was drilled in May/June 2018 from the saddle between the two summits of Belukha (49°48'27.7"N, 86°34'46.5"E, 4055 m asl.), the highest mountain in the Altai mountain range. The bedrock was reached and the total length of the core is 160 m. Three samples were analyzed from the deepest part (158-160 m). Seven, and three samples were analyzed from the deep parts of SLNS and Chongce, respectively. The SLNS ice core was retrieved in May 2010 from the south slope of the Shulenanshan Mountain (38°42'19.35"N, 97°15'59.70"E, 5337 m asl.). The bedrock was reached and the total length of the ice core is 81.05 m (Hou et al., submitted). The Chongce ice cap is located in the western Kunlun Mountains on the northwestern Tibetan Plateau, covering an area of 163.06 km$^2$ with a volume of 38.16 km$^3$. The ice analyzed in this study was sampled from Chongce Core 1, one of three ice cores drilled in October 2012 (35°14'5.77"N, 81°7'15.34"E, 6010 m asl.). Two of those cores reached bedrock with lengths of 133.8 m (Core 1) and 135.8 m (Core 2). In 2013, two more ice cores were recovered to bedrock with lengths of 216.6 m (Core 4) and 208.6 m (Core 5) at a higher altitude of 6100 m asl. (Hou et al., 2018). Find details about all samples in Table 1. No results from any of the cores analyzed in this study have been published previously.

All sample were decontaminated in a cold room (-20ºC) by cutting off the surface layer (~3 mm). Each sample was split into two parallel sections to perform both WIOC and DOC $^{14}C$ analysis. Samples for WIO$^{14}C$-dating were prepared following the protocol described in

https://doi.org/10.5194/tc-2020-234
Preprint. Discussion started: 2 September 2020


Uglietti et al. (2016) with a brief summary provided in the following. In order to remove potential contamination in the outer layer of the ice core, pre-cut samples from the inner part of the core were additionally rinsed with ultra-pure water (Sartorius, 18.2 MΩ×cm, TOC < 5ppb), resulting in samples masses ranging from ~300 to 600 g (Table 1). To dissolve carbonate potentially present in the ice, melted samples were acidified with HCl to pH < 2, before being sonicated for 5 min. Subsequently, the contained particles were filtered onto pre-baked (heated at 800 °C for 5 h) quartz fiber filters (Pallflex Tissueqtz-2500QAT-UP). In a second carbonate removal step, the filters were acidified 3 times with a total amount of 50 µL 0.2M HCl, left for 1 h, rinsed with 5 mL ultra-pure water and finally left again for drying. These initial steps were performed in a laminar flow box to ensure clean conditions. At the Laboratory for the Analysis of Radiocarbon with AMS (LARA) of the University of Bern the particle samples were then combusted in a thermo-optical OC/EC analyzer (Model4L, Sunset Laboratory Inc, USA) equipped with a non-dispersive infrared (NDIR) cell to quantify the $CO_2$ produced, using the well-established Swiss 4S protocol for OC/EC separation (Zhang et al., 2012). Being coupled to a 200 kV compact accelerator mass spectrometer (AMS, MIni CArbon DAting System MICADAS) equipped with a gas ion source via a Gas Interface System (GIS, Ruff et al., 2007; Synal et al., 2007, Szidat et al., 2014), the LARA Sunset-GIS-AMS system (Agrios et al., 2015; Agrios et al., 2017) allowed for final, direct online $^{14}C$ measurements of the $CO_2$ produced from the WIOC fraction.

For DO$^{14}$C analysis, sample preparation follows the procedure described in Fang et al. (2019). After transfer of pre-cut samples to the laboratory, samples were further decontaminated in the pre-cleaned melting vessel of the extraction setup by rinsing with ultrapure water before being melted, all performed under helium atmosphere. Simultaneously, a pre-cleaning step was applied to remove potential contamination in the system. For this, 50 mL ultra-pure water was injected into the reactor and acidified with 1 mL of 85% $H_3PO_4$. To enhance the oxidation efficiency, 2 mL of 100 ppm $FeSO_4$ and 1 mL of 50 mM $H_2O_2$ (Fenton's reagent) was also injected into the base water before turning on the UV lights for ~20 min, thereby monitoring the process via the online NDIR $CO_2$ analyzer. After the ice melted, the meltwater was filtrated under helium atmosphere, using a pre-baked in-line quartz fiber filter. The sample volume was determined by measuring the reactor fill level. The filtrate was acidified by mixing with the pre-treated base water. After degassing of $CO_2$ from inorganic carbon was completed as monitored by the $CO_2$- detector, 1 mL of 50 mM $H_2O_2$ was injected into the reactor right before the irradiation started. During UV oxidation, water vapor was

https://doi.org/10.5194/tc-2020-234
Preprint. Discussion started: 2 September 2020


removed by cryogenic trapping at -60 °C and produced $CO_2$ was trapped in liquid nitrogen. All steps were carried out under a constant flow of helium. The sample $CO_2$ was further cleaned from residual water vapor and quantified manometrically before being sealed into a glass vial for offline $^{14}C$ analyses. The $CO_2$ gas from DOC in the glass vial was directly injected into the MICADAS using a cracking system for glass vials under vacuum, allowing to then carry the $CO_2$ gas in a helium flow to the AMS ion source (Wacker et al., 2013).

All $^{14}C$ results are expressed as fraction modern ($F^{14}C$), which is the $^{14}C/^{12}C$ ratio of the sample divided by the same ratio of the modern standard referenced to the year 1950 (NIST, SRM 4990C, oxalic acid II), both being normalized to -25‰ in $\delta^{13}C$ to account for isotopic fractionation. All AMS $F^{14}C$ values presented here are finally corrected for the system and method characteristic contributions as reported previously (e.g. Uglietti et al., 2016 and Fang et al., 2019). For WIOC analysis using the Sunset-GIS-AMS system this includes a correction for the system background, i.e. constant contamination (0.91±0.18 µgC with $F^{14}C$ of 0.72±0.11). For the cracking system applied for DOC samples the constant contamination is 0.06±0.18 µgC with $F^{14}C$ of 0.50 ±0.11). Further corrections applied account for the AMS cross contamination (0.2% of the previous sample), and procedure blanks (1.26±0.59 µgC with $F^{14}C$ of 0.69±0.15 for WIOC samples and 1.9±1.6 µgC with a $F^{14}C$ value of 0.68±0.13 for DOC samples) All uncertainties were propagated throughout data processing until final $^{14}C$ calibration. These corrections, have a larger effect on low carbon mass samples (higher noise-to-sample ratio), resulting in a larger dating uncertainty. Therefore, we only discuss samples with a carbon mass larger than 10 µg as recommended in Uglietti et al. (2016). Radiocarbon ages are calculated following the law of radioactive decay using 5570 years as the half-life of radiocarbon, thus age equals -8033 * ln ($F^{14}C$) with -8033 years being Libby's mean lifetime of radiocarbon. Radiocarbon ages are given in years before present (BP) with the year of reference being 1950 (Stuiver and Polach, 1977). To obtain calibrated $^{14}C$ ages, the online program OxCal v4.3.2 with the IntCal13 radiocarbon calibration curve was used (Reimer et al., 2013; Ramsey, 2017). Calibrated ages, also given in years before present, are indicated with (cal BP) and denote the 1σ range unless stated otherwise.

## 3 Results

### 3.1 DOC and WIOC concentrations

https://doi.org/10.5194/tc-2020-234
Preprint. Discussion started: 2 September 2020


DOC concentrations are generally higher compared to the corresponding WIOC concentrations (Figure 2). For all samples from the four glaciers, the DOC/WIOC concentration ratio ranges from 1.2 to 4.0 with an average of 1.9 ± 0.6 (Table 2). This is at the lower end of previously reported average DOC/WIOC ratios of 2-8 (Legrand et al., 2007; Legrand et al., 2013, Fang et al., in prep.). This is likely explained by temporal variability because most samples in this study are several thousand years old, whereas the literature data only covers the last few centuries, including values from the industrial period in which additional anthropogenic sources exist (e.g. fossil DOC precursors). It is interesting to note that the average DOC/WIOC ratio at Belukha (2.5) is higher compared to the other sites (Colle Gnifetti, SLNS and Chongce is 1.8, 1.7 and 1.6, respectively). Because the Belukha glacier is surround by extensive Siberian Forests, the higher ratio may be explained by particularly high emissions of biogenic volatile organic compounds. This is corroborated by the observation that DOC concentrations are highest at this site (241 ± 82 µg/kg) (Figure 2). Absolute concentrations of DOC and WIOC are slightly lower at Colle Gnifetti (112 ± 12 µg/kg and 63 ± 13 µg/kg, respectively) compared to the other three glaciers (Table 1 and 2). Mean DOC and WIOC concentrations in the ice from the Tibetan Plateau are 211±28 µg/kg and 123±19 µg/kg for SLNS and 156±40 µg/kg and 99±37 µg/kg for Chongce, respectively. These values are higher compared to the pre-industrial (PI) average values found in European Alpine glaciers, not only compared to the few samples from Colle Gnifetti of this study, but also to previously reported values from the Fiescherhorn glacier with PI-DOC of ~95 µg/kg (Fang et al., in prep.) and PI-WIOC of ~30 µg/kg (Jenk et al., 2006), respectively; and from Colle Gnifetti with PI-WIOC of ~30 µg/kg (Legrand et al., 2007; Jenk et al., 2006).

### 3.2 Radiocarbon results

For all four sites, $F^{14}C$ of both fractions (WIOC and DOC) decreases with depth, indicating the expected increase in age (Figure 2, Table 1 and 2). For three of the sites (Colle Gnifetti, Belukha and SLNS), the corresponding DOC and WIOC fractions yielded comparable $F^{14}C$ values. They scatter along the 1:1 ratio line and are significantly correlated (Pearson correlation coefficient r=0.987, $p < .01$, n=14) and both intercept (0.021 ± 0.033) and slope (1.036 ± 0.048) are not significantly different from 0 and 1, respectively (Figure 3a). Nevertheless, Figure 2 and Figure 3a suggest a slight systematic offset towards lower $F^{14}C$ values for WIOC compared to DOC, at least for higher $F^{14}C$ values. This is particularly obvious for the Chongce samples,

https://doi.org/10.5194/tc-2020-234
Preprint. Discussion started: 2 September 2020


characterized by a high mineral dust load (see discussion in Sect. 4.2) and for which $F^{14}C$ values of DOC and WIOC differ significantly.

For all sites, the calibrated $^{14}C$ ages from both fraction show an increase in age with depth (Table 3). The ages range from ~0.2 to 20 kyr cal BP for DOC and ~0.9 to 22 kyr cal BP for WIOC, respectively. In both fractions, the oldest age was derived for the sample from the deepest part of the Belukha ice core. Samples from Colle Gnifetti generally showed younger ages (< 2 kyr cal BP). The two ice cores from the Tibetan Plateau (SLNS and Chongce) cover a similar age span from ~0.2±0.1 to 5.5±0.3 kyr cal BP in the DOC fraction. $WIO^{14}C$ gave similar ages for the samples from SLNS (0.9±0.4 to 6.6±0.8 kyr cal BP), but for Chongce they resulted much older (3.1±0.7 to 11.0±1.7 kyr cal BP, see discussion in Section 4.2).

# 4 Discussion

## 4.1 Radiocarbon dating with the DOC fraction

In Table 3, we present the first radiocarbon dating results of ice using the DOC fraction, with the exception of one dating point being part of the dataset to establish the very recent, first complete chronology of the Mt. Hunter ice core, Alaska (same setup and methodology as described here, Fang et al., submitted). The DOC calibrated $^{14}C$ age of ice increases with depth for all four sites, as expected for undisturbed glacier archives from the accumulation zone. The fact that none of the samples analyzed in this study (n=17) resulted in super modern $F^{14}C$ values (> 1) and the obtained significant correlation between the $F^{14}C$ of WIOC and DOC (Sect. 3.2) and the resulting calibrated $^{14}C$ ages (Pearson $r = 0.988$, $p < .01$, n=14, Figure S1) represent strong evidence against the previously suggested $^{14}C$ in-situ production in the DOC fraction (May, 2009). With the new $DO^{14}C$ dating method an average dating uncertainty of around ±200 years was achieved for samples with an absolute carbon mass of 20-60 µg, if the ice is younger than ~6 ka (Table 2). This uncertainty mainly arises from the correction of the procedure blank introduced during sample treatment prior to AMS analysis contributing with 20 to 70 % to the final overall uncertainty. The contribution thereby depends on carbon mass (larger for small samples) and sample age (the larger the bigger the difference between sample and blank $F^{14}C$). See how the overall uncertainty of $F^{14}C$ decreases with higher carbon mass in Figure S2 (see Sect. 2 for details on blank corrections). For DOC concentrations observed in this study, an initial ice mass of about 250 g was required, with about 20-30 % of the ice being removed

https://doi.org/10.5194/tc-2020-234
Preprint. Discussion started: 2 September 2020


during the decontamination processes inside the DOC set-up, yielding ~200 g of ice available for final analysis. Our results confirmed that with this new technique, the required ice mass can thus be reduced by more than a factor of two compared to the mass needed for $^{14}C$ dating using the WIOC fraction (expected based on the previously reported DOC/WIOC concentration ratio, Sect. 3.1). Consequently, using the DOC instead of the WIOC fraction for $^{14}C$ dating, a higher dating precision can be achieved for samples of similar mass. An additional benefit is that the DOC extraction procedure allows monitoring to ensure complete removal of inorganic carbon (Sect. 2), i.e. interfering carbonate (see Sect. 4.2), leading to an improved accuracy.

### 4.2 Potential contribution of carbonates to $^{14}C$ of WIOC

As described in Section 3.2, no significant difference between $F^{14}C$ of DOC and WIOC was observed for the ice samples from Colle Gnifetti, Belukha and SLNS (Figure 3). However, the observed offset for the samples from Chongce glacier needs to be discussed. Previously published WIOC $^{14}C$ ages from the upper parts of the Chongce Cores 2 and 4, less than 2 and ~6 km away from Core 1, did show large scatter with no clear increase in age with depth for samples younger than 2 ka. It was speculated that this was at least partly caused by the exceptionally high loading of mineral dust on the WIOC filters (Hou et al., 2018). Such high mineral dust loading was also observed during filtration of the samples analyzed in this study. High mineral dust content in the ice can influence $^{14}C$ dating with WIOC in two ways, by affecting filtration through clogging of the filter and by potentially contributing with $^{14}C$-depleted carbon from carbonate, as has been discussed in most previous studies. They all concluded, that for dust levels typically observed in ice cores from high elevation glaciers, no significant bias is detectable for $^{14}C$ of WIOC, but it was of concern for the elemental carbon (EC) fraction combusted at higher temperatures during OC/EC separation. This fraction – as well as total carbon (TC) the sum of OC and EC – is thus not recommended to be used for radiocarbon dating (Jenk et al., 2006; Jenk et al., 2007; Jenk et al., 2009; Sigl et al., 2009; Uglietti et al., 2016). In case of similar age of the DOC and WIOC fraction, a contribution of $^{14}C$-depleted carbonate (low $F^{14}C$) to WIOC would result in an $F^{14}C$ offset between the two fractions and yield a slope value different from 1, since it most strongly affects high $F^{14}C$ values (i.e. younger samples). This can easily be understood by the concept of isotopic mass balance. Therefore, to test the hypothesis that incomplete removal of carbonate resulted in the $F^{14}C$ DOC-WIOC offset observed in our dataset, we estimated the carbonate removal efficiency of our procedure by applying an isotopic mass balance model. We thereby used the $Ca^{2+}$

https://doi.org/10.5194/tc-2020-234
Preprint. Discussion started: 2 September 2020


concentration in the samples as a tracer for calcium carbonate (for details see supplement).

The obtained average removal efficiency of ~96% would amount to a residual carbonate carbon mass on the filter of ~4 µgC on average (Table 4). The effect of this not entirely complete removal, can easily explain the $F^{14}C$ DOC-WIOC offset observed for the Chongce ice core samples. By accounting for the estimated carbonate contribution, the offset for these samples is significantly reduced to the level of scatter observed for the three other sites (Figure 3b; for an according Figure with calibrated $^{14}C$ ages instead of $F^{14}C$ see S1). Based on these model results, we are also confident to conclude that residual carbonate carbon is the most likely cause to explain the slight systematic $F^{14}C$ DOC-WIOC shift we observed for the other three sites. The old samples from Belukha contain the highest $Ca^{2+}$ concentrations in this study. With their origin in the Late Glacial or Glacial-to-Holocene transition period, these samples might not be comparable to the other samples in terms of mineral dust sources and transport. Their $Ca^{2+}$-to-carbonate ratio or the abundance of the more soluble form of bicarbonate can thus be assumed to be at least slightly different compared to the rest of the samples with the determined average removal efficiency thus yielding a slight underestimation for the samples from Belukha (estimated to rather be ~99%, see Supplement). In any case, our results confirm the findings of previous studies that the potential carbonate related bias for $^{14}C$ dating using WIOC is hardly detectable for ice samples with normal dust loading, typically being less than the analytical uncertainty (around 10-20% of the determined age, see supplement Figure S3). For example, Uglietti et al. (2016) did not detect such an effect when comparing dating results from $WIO^{14}C$ with ages from independent methods.

### 4.3 $DO^{14}C$ ages in the context of published chronologies

In the following we will discuss our new $DO^{14}C$ results in the context of ages from previous studies (Table 5, Figure 4). For final calibration of $^{14}C$ ages, most of those earlier studies took advantage of the assumption of sequential deposition in the archive, which seems very reasonable considering the deposition of annual snow layers on top of each other on the glacier surface. Particularly in case of relatively large analytical uncertainties compared to the age difference of the samples, the sequential deposition model can moderately constrain the probability distribution of the calibrated age range in each sample of the dataset. For consistency we applied the same calibration approach here by using the in-built OxCal sequence model (Ramsey, 2008). For all $DO^{14}C$ data presented in this study, there is no

https://doi.org/10.5194/tc-2020-234
Preprint. Discussion started: 2 September 2020


difference in the calibrated ages using the sequence model and the ages from the conventional calibration approach (Table 3). We obtained the oldest age of ~21 kyr cal BP for the bedrock ice at Belukha, indicating this glacier to be oldest and of Pleistocene origin (Figure 4). This is older than the previously reported age of ~11 kyr cal BP, which was retrieved for the ice core from Belukha West Plateau extracted in 2003 (B03) and not from the saddle as the 2018 core (B18) analyzed in this study (Aizen et al., 2016; Uglietti et al., 2016). However, the sample from B03 was from a depth 0.6-0.3 m above bedrock. The age range modeled for B03 at the same depth above bedrock as sampled in this study (0.5-0 m) is ~28 kyr cal BP with a very large uncertainty of ~15 kyr (Uglietti et al., 2016). Thus, our new age for the oldest ice at Belukha agrees well with this previous result, but yields a much better constrained age with a strongly reduced uncertainty of ±4 kyr. The two glaciers from the Tibetan Plateau (SLNS and Chongce) show very similar bottom ages of ~5-6 kyr cal BP, which is in agreement with the previously reported age range of Tibetan Plateau glaciers (Hou et al., 2018). The bottom age of Chongce Core 1 determined here (5.6 ± 0.3 kyr cal BP) is slightly younger than the previously reported bottom age in Core 2 (6.3 ± 0.3 kyr cal BP, Hou et al., 2018), which is likely related to the influence of residual carbonates on the latter (Section 4.2). The bottom most sample of the Colle Gnifetti 2015 (CG15) core could not be dated because the small amount of ice available yielded an insufficient carbon mass of <10 µg for $^{14}C$ analysis. Previous WIO$^{14}C$ dating of a core obtained at Colle Gnifetti in 2003 (CG03) also revealed ice of Pleistocene origin with the ice at bedrock being older than 15 kyr cal BP (Jenk et al., 2009). The age obtained in this study was much younger with 1.2 kyr cal BP, but in excellent agreement with the age of CG03 at similar depth (~74 m below surface). This is a clear indication that the CG15 ice core drilling did not reach bedrock.

## 5 Conclusion

In this study, we evaluated and successfully validated the DO$^{14}C$ dating technique by directly comparing with results from the well-established WIO$^{14}C$ dating method on parallel samples. Achieving this goal was not only analytically demanding but also highly challenging because of the very limited availability of the sampling material requiring ice in rather large quantities and spanning a wide range of ages. The obtained DO$^{14}C$ ages for four different Eurasian glaciers, ranging from 0.2 ± 0.2 to 20.3 ± 4.1 kyrs cal BP, agreed well with the respective

https://doi.org/10.5194/tc-2020-234
Preprint. Discussion started: 2 September 2020


366 WIO$^{14}$C ages (0.9 ± 0.4 to 22.5 ± 1.1 kyrs cal BP) and with previously published chronologies
367 from these ice core sites. This underlines the great potential for applying DO$^{14}$C analysis for
368 ice core dating. Effects of in-situ $^{14}$C production on DO$^{14}$C ages, as suspected in previous
369 studies, were not observed. Our data confirmed that pre-industrial DOC concentrations are
370 higher by a factor of about two than WIOC concentrations in high alpine ice cores. With the
371 new DO$^{14}$C dating method an average dating uncertainty of around ±200 years was achieved
372 for samples with an absolute carbon mass > 20 µg and ages up to ~6 ka. For DOC
373 concentrations observed in this study, an initial ice mass of about 250 g was required. The
374 sample mass can thus be reduced by more than a factor of two compared to the mass needed
375 for $^{14}$C dating using the WIOC fraction. Furthermore, the new DO$^{14}$C dating revealed a slight
376 age bias of the WIOC fraction towards older ages, which however was found to be significant
377 only for ice containing high concentrations of mineral dust and in particular if younger than
378 ~1000 years, in agreement with findings of previous studies. In any case, for this age range,
379 other independent dating methods exist and the use of these in combination with radiocarbon
380 ages in a glaciological flow model to derive a final ice core age-depth relationship provides
381 additional constraint, thus reducing potential bias, for these younger ice sections (less weight
382 given to the potentially biased radiocarbon ages in this range). Nevertheless, future work for
383 improving the carbonate removal procedure is encouraged to further increase the accuracy of
384 $^{14}$C dating with the WIOC fraction.

385 In summary the main benefits of DO$^{14}$C dating of glacier ice compared to WIO$^{14}$C dating are
386 the reduced ice amount required, or higher precision for the same sample mass. The DOC
387 fraction is not affected from potential carbonate bias from mineral dust with the applied
388 methodology and thus ensures high dating accuracy. This new dating method opens up new
389 fields for radiocarbon dating of ice for example from remote or Polar Regions, where
390 concentrations of organic impurities in the ice are particularly low. Compared to the WIO$^{14}$C
391 dating, a downside is the more demanding and time consuming DOC extraction procedure and
392 because of its higher solubility, the higher mobility of DOC in case of meltwater, thus only
393 being applicable for dating ice which had been cold throughout its “lifetime”.

394

395 **Acknowledgements**

396 We thank Johannes Schindler for his great work in designing and building the DOC extraction
397 system and the two drilling teams on Colle Gnifetti and Belukha for collecting high quality ice

https://doi.org/10.5194/tc-2020-234
Preprint. Discussion started: 2 September 2020


cores. We acknowledge funding from the Swiss National Science Foundation (SNF) for the Sinergia project Paleo fires from high-alpine ice cores (154450), which allowed ice core drilling on Colle Gnifetti and Belukha, and for the project Reconstruction of pre-industrial to industrial changes of organic aerosols from glacier ice cores (200021_182765). We acknowledge the funding from the National Natural Science Foundation of China (91837102, 41830644) for the Tibetan ice core drilling. We dedicate this study to Alexander Zapf, who died tragically while climbing in the Swiss Alps, before he could fulfil his dream of ice dating with DO$^{14}$C.

## Data availability

The data is provided in the Tables.

## Author contributions

LF and TS performed $^{14}$C analysis. LF, TS, TMJ, and MS wrote the manuscript while all authors contributed to the discussion of the results. MS designed the study.

## Competing interests

The authors declare that they have no conflict of interest.

https://doi.org/10.5194/tc-2020-234
Preprint. Discussion started: 2 September 2020




## References

Agrios, K., Salazar, G., Zhang, Y.-L., Uglietti, C., Battaglia, M., Luginbühl, M., Ciobanu, V. G., Vonwiller, M. and Szidat, S.: Online coupling of pure $O_2$ thermo-optical methods–$^{14}C$ AMS for source apportionment of carbonaceous aerosols, Nucl. Instrum. Methods Phys. Res. B., 361, 288-293, https://doi.org/10.1016/j.nimb.2015.06.008, 2015.

Agrios, K., Salazar, G. and Szidat, S.: A Continuous-Flow Gas Interface of a Thermal/Optical Analyzer With $^{14}C$ AMS for Source Apportionment of Atmospheric Aerosols, Radiocarbon, 59, 921-932, https://doi.org/10.1017/RDC.2016.88, 2017.

Aizen, E. M., Aizen, V. B., Takeuchi, N., Mayewski, P. A., Grigholm, B., Joswiak, D. R., Nikitin, S. A., Fujita, K., Nakawo, M. and Zapf, A.: Abrupt and moderate climate changes in the mid-latitudes of Asia during the Holocene, J. Glaciol., 62, 411-439, https://doi.org/10.1017/jog.2016.34, 2016.

Bolzan, J. F.: Ice flow at the Dome C ice divide based on a deep temperature profile, J. Geophys. Res. Atmos., 90, 8111-8124, https://doi.org/10.1029/JD090iD05p08111, 1985.

ChongYi, E., Sun, Y., Li, Y. and Ma, X., The atmospheric composition changes above the West Kunlun Mountain, Qinghai-Tibetan Plateau, International Conference on Civil, Transportation and Environment, Atlantis Press, 2016.

Fang, L., Schindler, J., Jenk, T., Uglietti, C., Szidat, S. and Schwikowski, M. J. R.: Extraction of Dissolved Organic Carbon from Glacier Ice for Radiocarbon Analysis, Radiocarbon, 61, 681-694, https://doi.org/10.1017/RDC.2019.36, 2019.

Fang L., Winski D., Kreutz K., Jenk T.M., Schwikowski M., Osterberg E., Campbell S., Wake C., $^{14}C$ age constraints in the Mt. Hunter, Alaska ice core: implications for chronology and early Holocene Arctic ice extent, submitted to Journal of Glaciology.

Fang L., Cao F., Jenk T. M., Vogel A. L., Zhang Y.L., Wacker L., Salazar G., Szidat S., Schwikowski M.: Enhancement of carbonaceous aerosol during the 20th century by anthropogenic activities: insights from an Alpine ice core, in preparation.

Hou, S., Jenk, T. M., Zhang, W., Wang, C., Wu, S., Wang, Y., Pang, H. and Schwikowski, M. J. T. C.: Age ranges of the Tibetan ice cores with emphasis on the Chongce ice cores, western Kunlun Mountains, The Cryosphere, 12, 2341-2348, https://doi.org/10.5194/tc-12-2341-2018, 2018.

Hou, S., Zhang W., Fang L., Jenk T.M., Wu S., Pang H., Schwikowski M., Brief Communication: New evidence further constraining Tibetan ice core chronologies to the Holocene, Submitted to The Cryosphere.

Jenk, T. M., Szidat, S., Schwikowski, M., Gaggeler, H. W., Brutsch, S., Wacker, L., Synal, H. A. and Saurer, M.: Radiocarbon analysis in an Alpine ice core: record of anthropogenic and biogenic contributions to carbonaceous aerosols in the past (1650-1940), Atmos. Chem. Phys., 6, 5381-5390, 2006.

Jenk, T. M., Szidat, S., Schwikowski, M., Gäggeler, H., Wacker, L., Synal, H.-A. and Saurer, M.: Microgram level radiocarbon ($^{14}C$) determination on carbonaceous particles in ice, Nucl. Instrum. Methods Phys. Res. B., 259, 518-525, https://doi.org/10.1016/j.nimb.2007.01.196, 2007.

Jenk, T. M., Szidat, S., Bolius, D., Sigl, M., Gaeggeler, H. W., Wacker, L., Ruff, M., Barbante, C., Boutron, C. F. and Schwikowski, M.: A novel radiocarbon dating technique applied to an ice core from the Alps indicating late Pleistocene ages, J Geophys. Res. Atmos., 114, https://doi.org/10.1029/2009JD011860, 2009.


458 Lal, D., Jull, A. T., Burr, G. and Donahue, D.: Measurements of in situ $^{14}C$ concentrations in Greenland
459 Ice Sheet Project 2 ice covering a 17 - kyr time span: Implications to ice flow dynamics, J. Geophys.
460 Res. Oceans, 102, 26505-26510, https://doi.org/10.1029/96JC02224, 1997.

461 Legrand, M., Preunkert, S., Schock, M., Cerqueira, M., Kasper-Giebl, A., Afonso, J., Pio, C., Gelencsér,
462 A. and Dombrowski-Etchevers, I.: Major 20th century changes of carbonaceous aerosol components
463 (EC, WinOC, DOC, HULIS, carboxylic acids, and cellulose) derived from Alpine ice cores, J. Geophys.
464 Res. Atmos., 112, https://doi.org/10.1029/2006JD008080, 2007.

465 Legrand, M., Preunkert, S., Jourdain, B., Guilhermet, J., Fain, X., Alekhina, I. and Petit, J. R.: Water-
466 soluble organic carbon in snow and ice deposited at Alpine, Greenland, and Antarctic sites: a critical
467 review of available data and their atmospheric relevance, Clim. Past Discuss., 9, 2357-2399,
468 doi:10.5194/cpd-9-2357-2013, 2013.

469 Licciulli, C., Bohleber, P., Lier, J., Gagliardini, O., Hoelzle, M. and Eisen, O.: A full Stokes ice-flow
470 model to assist the interpretation of millennial-scale ice cores at the high-Alpine drilling site Colle
471 Gnifetti, Swiss/Italian Alps, J. Glaciol., 66, 35-48, https://doi.org/10.1017/jog.2019.82, 2020.

472 May, B. L. Radiocarbon microanalysis on ice impurities for dating of Alpine glaciers, Ph.D. thesis,
473 University of Heidelberg, Germany, 127pp., 2009.

474 May, B., Wagenbach, D., Hoffmann, H., Legrand, M., Preunkert, S. and Steier, P.: Constraints on the
475 major sources of dissolved organic carbon in Alpine ice cores from radiocarbon analysis over the
476 bomb - peak period, J. Geophys. Res. Atmos., 118, 3319-3327, https://doi.org/10.1002/jgrd.50200,
477 2013.

478 Nye, J.: On the theory of the advance and retreat of glaciers, Geophys. J. Int., 7, 431-456, 1963.

479 Ramsey, C. B.: Deposition models for chronological records, Quat. Sci. Rev., 27, 42-60,
480 https://doi.org/10.1016/j.quascirev.2007.01.019, 2008.

481 Ramsey, C. B.: Methods for summarizing radiocarbon datasets, Radiocarbon, 59, 1809-1833,
482 https://doi.org/10.1017/RDC.2017.108, 2017.

483 Reimer, P. J., Bard, E., Bayliss, A., Beck, J. W., Blackwell, P. G., Ramsey, C. B., Buck, C. E., Cheng, H.,
484 Edwards, R. L., Friedrich, M., Grootes, P., Guilderson, T., Haflidason, H., Hajdas, I., Hatté, C., Heaton,
485 T., Hoffmann, D. L., Hogg, A. G., Hughen, K. A., Felix Kaiser, K., Kromer, B., Manning, S. W., Niu, M.,
486 Reimer, R. W., Richards, D. A., Scott, E. M., Southon, J. R., Staff, R. A., Turney, C. S. and van der Plicht,
487 J.: IntCal13 and Marine13 radiocarbon age calibration curves 0–50,000 years cal BP, Radiocarbon, 55,
488 1869-1887, https://doi.org/10.2458/azu_js_rc.55.16947, 2013.

489 Ruff, M., Wacker, L., Gäggeler, H., Suter, M., Synal, H.-A. and Szidat, S.: A gas ion source for
490 radiocarbon measurements at 200 kV, Radiocarbon 49, 307-314,
491 https://doi.org/10.1017/S0033822200042235, 2007.

492 Sigl, M., Jenk, T. M., Kellerhals, T., Szidat, S., Gäggeler, H. W., Wacker, L., Synal, H.-A., Boutron, C.,
493 Barbante, C. and Gabrieli, J.: Towards radiocarbon dating of ice cores, J. Glaciol., 55, 985-996,
494 https://doi.org/10.3189/002214309790794922, 2009.

495 Smith, A., Levchenko, V., Etheridge, D., Lowe, D., Hua, Q., Trudinger, C., Zoppi, U. and Elcheikh, A.: In
496 search of in-situ radiocarbon in Law Dome ice and firn, Nucl. Instrum. Methods Phys. Res. B., 172,
497 610-622, https://doi.org/10.1016/S0168-583X(00)00280-9, 2000.



498 Steier, P., Fasching, C., Mair, K., Liebl, J., Battin, T., Priller, A. and Golser, R., A new UV oxidation
499 setup for small radiocarbon samples in solution. Radiocarbon, 55, 373-382, DOI:
500 10.2458/azu_js_rc.55.16368, 2013.

501 Stuiver, M. and Polach, H. A.: Discussion reporting of $^{14}C$ data, Radiocarbon 19, 355-363, 1977.

502 Synal, H.-A., Stocker, M. and Suter, M.: MICADAS: a new compact radiocarbon AMS system, Nucl.
503 Instrum. Methods Phys. Res. B., 259, 7-13, https://doi.org/10.1016/j.nimb.2007.01.138, 2007.

504 Szidat, S., Salazar, G. A., Vogel, E., Battaglia, M., Wacker, L., Synal, H.-A. and Türler, A.: $^{14}C$ analysis
505 and sample preparation at the new Bern Laboratory for the Analysis of Radiocarbon with AMS
506 (LARA), Radiocarbon, 56, 561-566, 10.2458/56.17457,2014.

507 Thompson, L. G., Tandong, Y., Davis, M. E., Mosley-Thompson, E., Mashiotta, T. A., Lin, P.-N.,
508 Mikhalenko, V. N. and Zagorodnov, V. S. J. A. o. G.: Holocene climate variability archived in the
509 Puruogangri ice cap on the central Tibetan Plateau, Ann. Glaciol., 43, 61-69,
510 https://doi.org/10.3189/172756406781812357, 2006.

511 Uglietti, C., Zapf, A., Jenk, T. M., Sigl, M., Szidat, S., Salazar Quintero, G. A. and Schwikowski, M.:
512 Radiocarbon dating of glacier ice: overview, optimisation, validation and potential, The Cryosphere
513 10, 3091-3105, 10.5194/tc-10-3091-2016, 2016.

514 Van de Wal, R., Van Roijen, J., Raynaud, D., Van der Borg, K., De Jong, A., Oerlemans, J., Lipenkov, V.
515 and Huybrechts, P.: From $^{14}C/^{12}C$ measurements towards radiocarbon dating of ice. Tellus B Chem.
516 Phys. Meteorol., 46, 91-102, https://doi.org/10.3402/tellusb.v46i2.15755, 1994.

517 Wacker, L., Fahrni, S. M., Hajdas, I., Molnar, M., Synal, H. A., Szidat, S. and Zhang, Y. L.: A versatile gas
518 interface for routine radiocarbon analysis with a gas ion source, Nucl. Instrum. Methods Phys. Res.
519 B., 294, 315-319, https://doi.org/10.1016/j.nimb.2012.02.009, 2013.

520 Woon, D. E.: Modeling gas-grain chemistry with quantum chemical cluster calculations. I.
521 Heterogeneous hydrogenation of CO and $H_2CO$ on icy grain mantles. The Astrophys. J., 569, 541-548,
522 2002.

523 Zhang, Y. L., Perron, N., Ciobanu, V. G., Zotter, P., Minguillón, M. C., Wacker, L., Prévôt, A. S. H.,
524 Baltensperger, U. and Szidat, S.: On the isolation of OC and EC and the optimal strategy of
525 radiocarbon-based source apportionment of carbonaceous aerosols, Atmos. Chem. Phys., 12, 10841-
526 10856, https://doi.org/10.5194/acp-12-10841-2012, 2012.

527

528

https://doi.org/10.5194/tc-2020-234
Preprint. Discussion started: 2 September 2020




**Table 1** WIOC samples analyzed from Colle Gnifetti, Belukha, SLNS and Chongce ice cores.

| Core section | Depth (m) | Ice mass (kg) | WIOC (µg) | Concentration (µg/kg) | Bern AMS Nr. | $F^{14}C$ (±1σ) | $^{14}C$ age (BP, ±1σ) |
|---|---|---|---|---|---|---|---|
| CG110 | 72.1-72.7 | 0.570 | 35.2 | 61.9±3.3 | 11770.1.1 | 0.875±0.011 | 1073±105 |
| CG111 | 72.7-73.4 | 0.539 | 38.7 | 71.8±3.8 | 11771.1.1 | 0.848±0.010 | 1321±101 |
| CG112 | 73.4-73.9 | 0.536 | 23.7 | 44.1±2.4 | 11772.1.1 | 0.852±0.014 | 1284±143 |
| CG113 | 73.9-74.6 | 0.549 | 39.8 | 72.4±3.8 | 11773.1.1 | 0.786±0.010 | 1937±109 |
| Belukha412 | 158.3-159.0 | 0.443 | 37.8 | 85.2±4.5 | 11766.1.1 | 0.367±0.009 | 8055±189 |
| Belukha414 | 159.5-160.3 | 0.336 | 27.8 | 82.6±4.4 | 11768.1.1 | 0.212±0.012 | 12473±534 |
| Belukha415 | 160.3-160.9 | 0.319 | 39.3 | 123.3±6.5 | 11769.1.1 | 0.100±0.010 | 18462±896 |
| SLNS101 | 56.8-57.5 | 0.420 | 41.5 | 98.9±2.1 | 12325.1.1 | 0.902±0.047 | 825±420 |
| SLNS113 | 64.7-65.4 | 0.427 | 45.3 | 106.1±2.5 | 12324.1.1 | 0.852±0.046 | 1284±438 |
| SLNS122 | 68.9-69.7 | 0.424 | 58.5 | 138.0±3.6 | 12323.1.1 | 0.807±0.046 | 1727±4459 |
| SLNS127 | 71.8-72.5 | 0.483 | 50.9 | 105.3±2.5 | 12322.1.1 | 0.695±0.046 | 2921±531 |
| SLNS136 | 76.7-77.5 | 0.374 | 50.6 | 135.2±3.0 | 12321.1.1 | 0.521±0.046 | 5235±704 |
| SLNS139 | 78.9-79.6 | 0.485 | 61.2 | 126.3±3.6 | 12320.1.1 | 0.521±0.045 | 5232±701 |
| SLNS141-142 | 80.3-81.0 | 0.413 | 61.7 | 149.5±3.8 | 12319.1.1 | 0.489±0.046 | 5754±748 |
| CC237 | 126.0-126.7 | 0.352 | 22.4 | 63.7±1.8 | 12328.1.1 | 0.704±0.049 | 2815±554 |
| CC244 | 130.2-130.8 | 0.311 | 29.8 | 95.9±2.2 | 12327.1.1 | 0.639±0.048 | 3602±599 |
| CC252 | 133.4-133.8 | 0.174 | 23.8 | 136.7±4.3 | 12326.1.1 | 0.316±0.049 | 9256±1240 |

https://doi.org/10.5194/tc-2020-234
Preprint. Discussion started: 2 September 2020




**Table 2** DOC samples analyzed for Colle Gnifetti, Belukha, SLNS and Chongce ice cores.

| Core section | Depth (m) | Ice mass (kg) | DOC (µg) | Concentration (µg/kg) | Bern AMS Nr. | $F^{14}C$ (±1σ) | $^{14}C$ age (BP, ±1σ) | DOC/ WIOC |
|---|---|---|---|---|---|---|---|---|
| CG110 | 72.1-72.7 | 0.171 | 18.9 | 110.0±2.7 | 11575.1.1 | 0.943±0.030 | 474±259 | 1.8 |
| CG111 | 72.7-73.4 | 0.207 | 25.5 | 122.9±3.0 | 11576.1.1 | 0.901±0.021 | 836±190 | 1.7 |
| CG112 | 73.4-73.9 | 0.248 | 23.6 | 95.0±2.3 | 11577.1.1 | 0.889±0.021 | 943±192 | 2.2 |
| CG113 | 73.9-74.6 | 0.246 | 29.5 | 119.4±2.9 | 11578.1.1 | 0.849±0.016 | 1312±151 | 1.7 |
| Belukha412 | 158.3-159.0 | 0.172 | 28.5 | 165.0±4.0 | 11581.1.1 | 0.315±0.024 | 9284±623 | 1.9 |
| Belukha414 | 159.5-160.3 | 0.128 | 41.9 | 327.4±7.9 | 11584.1.1 | 0.239±0.019 | 11505±648 | 4.0 |
| Belukha415 | 160.3-160.9 | 0.102 | 23.7 | 231.0±5.6 | 11585.1.1 | 0.144±0.041 | 15584±2298 | 1.9 |
| SLNS101 | 56.8-57.5 | 0.238 | 44.0 | 184.9±4.5 | 12458.1.1 | 0.972±0.016 | 227±131 | 1.9 |
| SLNS113 | 64.7-65.4 | 0.213 | 39.4 | 185.2±4.5 | 12459.1.1 | 0.942±0.016 | 484±137 | 1.7 |
| SLNS122 | 68.9-69.7 | 0.234 | 57.9 | 248.0±6.0 | 12460.1.1 | 0.773±0.010 | 2073±101 | 1.8 |
| SLNS127 | 71.8-72.5 | 0.183 | 57.8 | 229.7±5.5 | 12461.1.1 | 0.730±0.009 | 2527±101 | 2.2 |
| SLNS136 | 76.7-77.5 | 0.220 | 48.3 | 219.1±5.3 | 12462.1.1 | 0.657±0.009 | 3380±112 | 1.6 |
| SLNS139 | 78.9-79.6 | 0.208 | 48.1 | 230.8±5.6 | 12463.1.1 | 0.580±0.010 | 4381±131 | 1.8 |
| SLNS141-142 | 80.3-81.0 | 0.246 | 43.8 | 177.5±4.3 | 12464.1.1 | 0.550±0.025 | 4809±151 | 1.2 |
| CC237 | 126.0-126.7 | 0.208 | 28.5 | 136.6±3.3 | 12454.1.1 | 0.980±0.023 | 161±185 | 2.1 |
| CC244 | 130.2-130.8 | 0.167 | 21.7 | 129.8±3.1 | 12455.1.1 | 0.800±0.018 | 1789±185 | 1.4 |
| CC252 | 133.4-133.8 | 0.120 | 24.3 | 202.5±4.9 | 12456.1.1 | 0.546±0.016 | 4854±239 | 1.5 |

https://doi.org/10.5194/tc-2020-234
Preprint. Discussion started: 2 September 2020




**Table 3** Calibrated WIO$^{14}$C and DO$^{14}$C ages using OxCal v4.3.2 with the Intcal13 radiocarbon calibration curve. Ages are given as the OxCal provided μ-age ± 1σ, which is the calibrated mean age accounting for the age probability distribution. In addition, calibrated ages derived when applying the OxCal sequence deposition model for further constraint are shown.

| Core section | WIOC Cal age (cal BP) | WIOC Cal age with sequence (cal BP) | DOC Cal age (cal BP) | DOC Cal age with sequence (cal BP) |
|---|---|---|---|---|
| CG110 | 1024±110 | 1003±99 | 464±235 | 403±196 |
| CG111 | 1238±96 | 1198±81 | 810±169 | 749±123 |
| CG112 | 1209±130 | 1310±98 | 901±176 | 947±139 |
| CG113 | 1898±130 | 1890±123 | 1222±153 | 1248±144 |
| Belukha412 | 8957±265 | 8953±247 | 10695±867 | 10701±861 |
| Belukha414 | 14780±781 | 14741±691 | 13646±893 | 15063±737 |
| Belukha415 | 22485±1112 | 22343±949 | 20264±4073 | 20605±3936 |
| SLNS101 | 851±395 | 707±317 | 250±145 | 226±137 |
| SLNS113 | 1298±452 | 1264±333 | 480±131 | 505±111 |
| SLNS122 | 1775±513 | 1902±427 | 2057±129 | 2056±129 |
| SLNS127 | 3178±677 | 3223±625 | 2585±125 | 2585±125 |
| SLNS136 | 6033±829 | 5424±617 | 3635±138 | 3636±137 |
| SLNS139 | 6032±811 | 6171±567 | 5014±191 | 5007±187 |
| SLNS141-142 | 6619±841 | 7069±676 | 5519±188 | 5531±176 |
| CC237 | 3057±704 | 2956±564 | 237±151 | 233±153 |
| CC244 | 4050±764 | 4214±699 | 1737±211 | 1738±212 |
| CC252 | 10998±1689 | 10948±1656 | 5580±294 | 5580±295 |

https://doi.org/10.5194/tc-2020-234
Preprint. Discussion started: 2 September 2020


**Table 4** Estimated residual carbonate carbon on the analyzed WIOC filters. $Ca^{2+}$ concentrations, used here as a tracer for carbonates, are average values for the sampled ice core sections (or site if data not available) of which the mass is also indicated.

| Core section | $Ca^{2+}$ concentration (ppb) | ice sample mass (kg) | residual carbonate C (µgC) |
|---|---|---|---|
| CG110 | 100 | 0.570 | 0.3 |
| CG111 | 110 | 0.539 | 0.3 |
| CG112 | 61 | 0.536 | 0.2 |
| CG113 | 59 | 0.549 | 0.2 |
| Belukha412 | 4191 | 0.443 | 10.2 |
| Belukha414 | 7566 | 0.336 | 13.9 |
| Belukha415 | 3737 | 0.319 | 6.5 |
| SLNS101 | 1400* | 0.420 | 3.2 |
| SLNS113 | same | 0.427 | 3.3 |
| SLNS122 | same | 0.424 | 3.3 |
| SLNS127 | same | 0.483 | 3.7 |
| SLNS136 | same | 0.374 | 2.9 |
| SLNS139 | same | 0.485 | 3.7 |
| SLNS141-142 | same | 0.413 | 3.2 |
| CC237 | 2170[#] | 0.352 | 4.2 |
| CC244 | same | 0.311 | 3.7 |
| CC252 | same | 0.174 | 2.1 |

*No $Ca^{2+}$ concentrations are available for SLNS, instead the average $Ca^{2+}$ concentration over the last 7000 years measured on the nearby Puruogangri ice cap on the central Tibetan Plateau are used here(Thompson et al., 2006).

[#] $Ca^{2+}$ concentration over the period of 1903-1992 from another core drilled on the Chongce ice cap by a different group (ChongYi et al., 2016).

https://doi.org/10.5194/tc-2020-234
Preprint. Discussion started: 2 September 2020




**Table 5** $DO^{14}C$ dating results for near bedrock ice compared to results from previous studies (visualized in Figure 4).

| Site | Study | Core | Dating method | Depth above bedrock (m) | Age (cal BP) |
|---|---|---|---|---|---|
| Colle Gnifetti | this study | CG15 | $DO^{14}C$ | (74.3 m below surface)* | 1248 ± 144 |
| | Jenk et al., 2009 | CG03 | $WIO^{14}C$ | (73.5 m below surface)# | 1152 ± 235 |
| | Jenk et al., 2009 | CG03 | Model | (74.3 m below surface)& | $1160 \pm^{140}_{170}$ |
| | Jenk et al., 2009 | CG03 | $WIO^{14}C$ | 0.6-0 | >15000 |
| | Jenk et al., 2009 | CG03 | Model | oldest ice estimate | $19100 \pm^{4800}_{4500}$ |
| Belukha | this study | B18 (saddle) | $DO^{14}C$ | 0.5-0 | 20605 ± 3936 |
| | Aizen et al., 2016 | B03 (west plateau) | $WIO^{14}C$ | 0.6-0.3 | 11015 ± 1221 |
| | Uglietti et al., 2016 | B03 (west plateau) | Model | 0.6-0 | 28500 ± 16200 |
| SLNS | this study | SLNS | $DO^{14}C$ | 0.4-0 | 5531 ± 176 |
| | no previous results | | --- | --- | --- |
| Chongce | this study | Core 1 | $DO^{14}C$ | 0.2-0 | 5580 ± 295 |
| | Hou et al., 2018 | Core 2 | $WIO^{14}C$ | 1.2-0.8 | 6253 ± 277 |
| | Hou et al., 2018 | Core 2 | Model | oldest ice estimate | $9000 \pm^{7900}_{3600}$ |

*precise bedrock depth unknown at this coring site, #sampled depth being closest to depth sampled in this study, &modeled age at same depth as sampled in this study.

https://doi.org/10.5194/tc-2020-234
Preprint. Discussion started: 2 September 2020




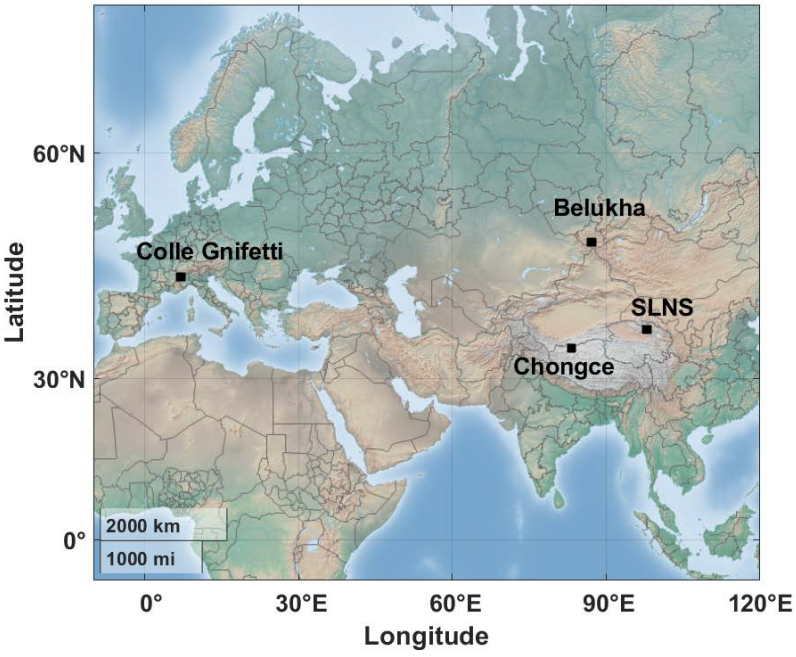


**Figure 1:** Location of the four glaciers Colle Gnifetti, Belukha, Chongce, and Shu Le Nan Shan (SLNS). Map made from Matlab R2019b geobasemap. Colle Gnifetti is located in the Monte Rosa massif in the Swiss Alps, Belukha glacier in the Altai mountain range, Russia, the Chongce ice cap on the northwestern Tibetan Plateau, China, and the SLNS at the south slope of the Shulenanshan Mountain, China.

https://doi.org/10.5194/tc-2020-234
Preprint. Discussion started: 2 September 2020


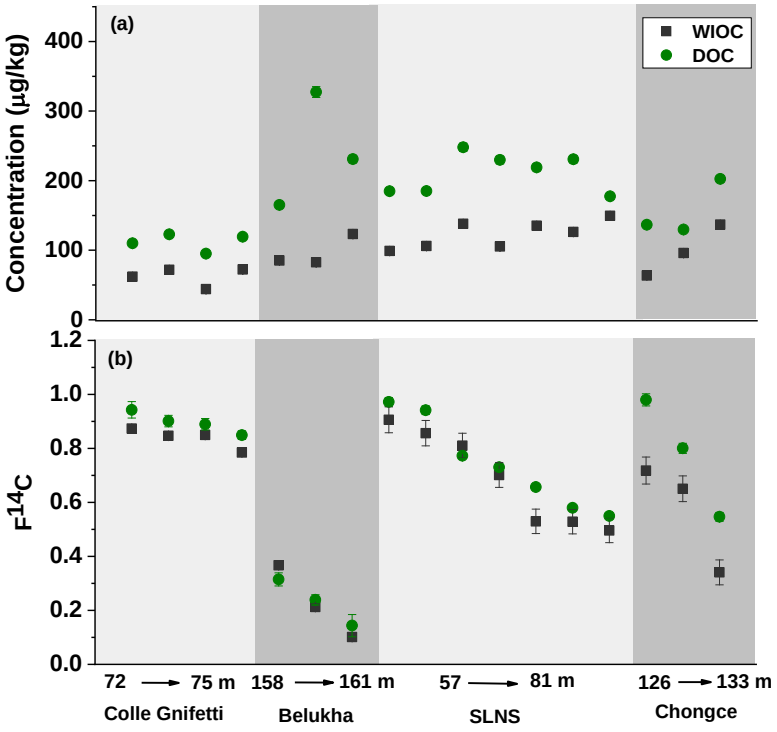


**Figure 2**: Comparison of results from the WIOC and DOC fractions for the studied four sites. (a) concentrations (b) $F^{14}C$. The error bars denote the overall analytical 1σ uncertainty.

https://doi.org/10.5194/tc-2020-234
Preprint. Discussion started: 2 September 2020




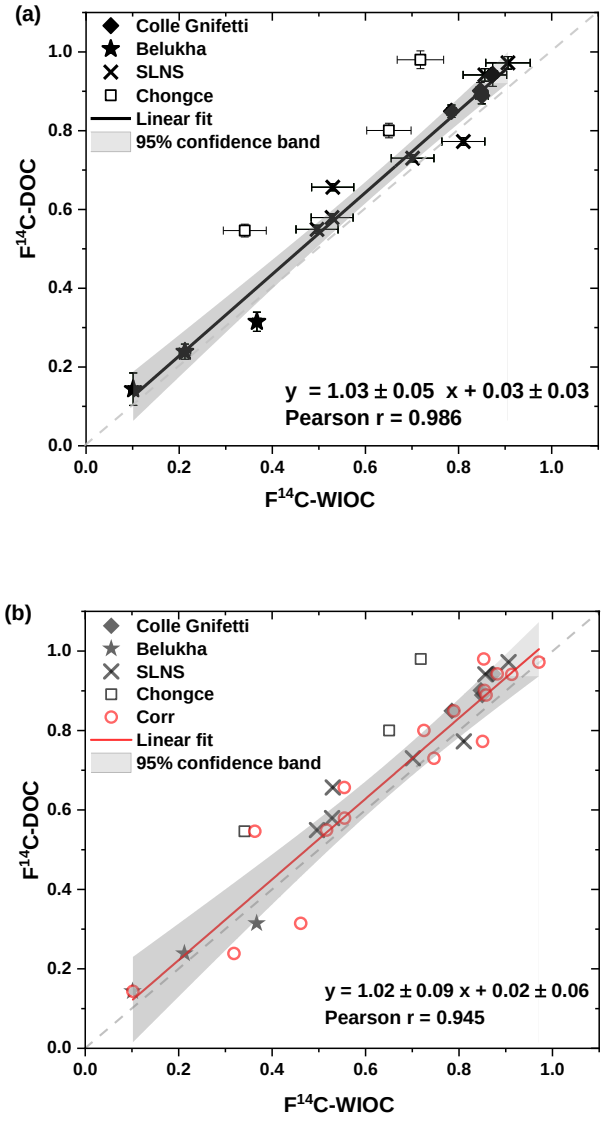


**Figure 3:** Scatter plot showing the correlation between $F^{14}C$ of WIOC and DOC. (a) Measured values for the four sites (see legend). For the linear fit shown, the data from Chongce (open symbols) was not included. (b) Same data as in (a) but additionally with $F^{14}C$-WIOC after accounting for the modeled residual carbonate carbon contribution (red open dots). Different to (a), the data from Chongce was here included for the linear fit (red line). The shaded area indicates the confidence band.

https://doi.org/10.5194/tc-2020-234
Preprint. Discussion started: 2 September 2020




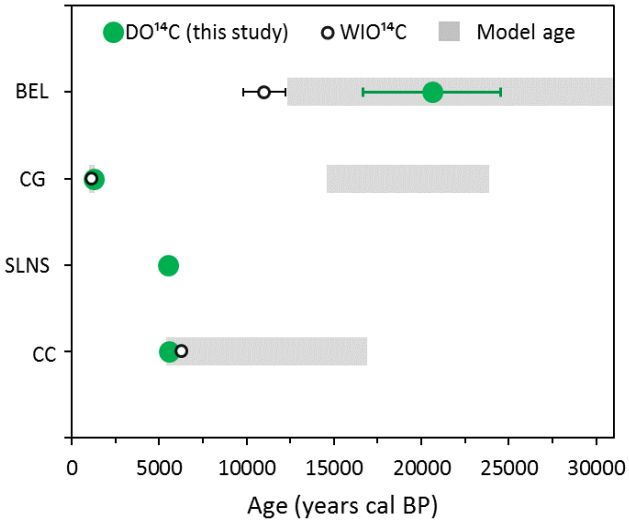


**Figure 4** Age of ice at the very bottom of the four glaciers (close to bedrock). DO$^{14}$C dates are shown with filled squares and previous reported WIO$^{14}$C ages indicated by open circles. The modeled estimate of the Belukha bottom age (gray bar) is from Uglietti et al. (2016). The modeled Colle Gnifetti bottom age from Jenk et al. (2009) and the indicated WIO$^{14}$C value is from ice sampled from the CG03 core at similar depth as in this study. For Chongce, the result of the deepest WIOC sample from core 2 is shown together with the modelled bottom age (Hou et al., 2018). Find all data and information summarized in Table 5.